



Comparison of catalysis of ethanol and methanol electro-oxidation by layered Pt/GO-ZSM-5 over graphite foil for fuel cell applications

Basu M. Daas^{1*}, Susanta Ghosh²

¹Department of Chemistry, Government Degree College, Dharmanagar, Tripura, India.

²Integrated Science Education & Research Centre, Visva-Bharati, Santiniketan, W. B., India.

Abstract : Platinum nanoparticles electro-deposited on graphene oxide over carbon felt electrodes are found to be able to catalyse electro-oxidation reactions of fuel cells. But as zeolites have added advantages of a support and second catalyst so this investigation can prove important. An interesting investigation of influence of platinum nanoparticles electro-deposited on 1:1 composite of graphene oxide and zeolite over carbon felt electrodes in electro-catalysis of ethanol and methanol is done. The results show a promising improvement in the catalytic ability of platinum nanoparticles in presence of zeolite additive. The stability of the electrodes with composite of graphene oxide and zeolite is also found to be better. Thus zeolites can increase the ability and stability of catalysts of fuel cell reactions.

Keywords: Graphene oxide; ZSM-5; Zeolite modified electrode; Platinum nanoparticles; Electro-oxidation; Fuel cell.

1. Introduction:

Pt loaded reduced graphene oxide Pt/GO/C electrodes have catalytic activity towards electro-oxidation of ethanol [1]. But for commercial application of DEFC, the main hurdles are exorbitant cost of the noble metals as well as the inability of platinum to catalyse the fission of C-C bond and to cleanse the adsorbed carbon monoxide intermediate [2-4]. For maximum utilization of platinum by minimizing the cost, high surface area supporting materials are an alternative. Ideal support materials should contain considerable specific surface area, electrical conductivity and porosity [5,6].

GO is a cheaper alternative for pure platinum by dint of high specific surface area, with unique graphitized basal plane structure having excellent electrical, mechanical and thermal properties [7,8].

Graphene and reduced graphene oxide nanosheets are planar sp^2 hybridised 2d support materials, with high specific surface area and perfection in planar structure; excellent electrical, mechanical and thermal properties, and outstanding conductivity [8-13]. Unlike the traditional carbon materials the high specific surface area of graphene oxide is due to interrelated open channels of graphene layers and independent of pore distribution [14]. Electrochemical reduction of graphene oxide to reduced form and electro-deposition of platinum onto it is a hazardless, effective and controllable method [15]. In reduced GO, oxygen content is decreased and sp^2 hybridised carbon is restored resulting much better electrochemical capacitance and cycling durability [16].

But for commercial application of graphene oxide as a support material is the tendency to stack together by

strong inter-sheet π - π interactions which blocking the catalytic sites and thereby reducing the exposed surface area of GO, and resisting the diffusion of reactants to the electrode [6,17,18]. Moreover, during the drying process, the reduced graphene oxide sheets irreversibly agglomerate or restack through van der Waals interactions [19,20]. Furthermore, reduced graphene oxide sheets obtained by conventional methods possess more defects which hinder the electron transfer. Lastly, reduced graphene oxide is unfavourable for electrolyte dispersion within the layers [21,22].

Insertion of ZSM-5 within the individual sheets to resist the agglomeration and stacking tendency may be effective; the support material not only improves the homogeneous dispersion of reduced graphene oxide sheets but also lowers the defects [15,23-26].

2. Experimental details:

2.1. Materials and methods:

ZSM-5 and chloroplatinic acid hexahydrate ($\text{H}_2\text{PtCl}_6 \cdot 6\text{H}_2\text{O}$) used were of analytical grade. ZSM-5, with $\text{SiO}_2:\text{Al}_2\text{O}_3$ ratio of 30 ± 5 , Si:Al ratio of 38 and pore diameter of 5.3 - 5.8 Å (from Greenstone, Switzerland), chloroplatinic acid hexahydrate ($\text{H}_2\text{PtCl}_6 \cdot 6\text{H}_2\text{O}$) (from Sigma-Aldrich, USA), 98% pure graphite foil (G-foil) (from Alfa Aesar, USA), 99.9% pure graphite powder (from Alfa Aesar, USA), ethanol (from Changshu Yangyuan Chemical, China) and freshly triple-distilled water was used for all purposes and all experiments to prevent contamination of any sort.

Graphene oxide (GO) was prepared and then GO/G-foil and GO/ZSM-5/G-foil electrodes were prepared and their electro-catalytic behaviour on oxidation of 1 M ethanol in 0.5 M H_2SO_4 was investigated by model PGSTAT128N of Autolab cyclic voltammeter from Metrohm.

2.2. Preparation of electrodes:

2.2.1. Preparation of Graphite Oxide:

Graphite oxide was prepared by following Hummer's Method [27]. Into 40 mL concentrated H_2SO_4 , 1 g of graphite powder and 0.5 g of NaNO_3 were added at RT and stirred for 15 min in ice-bath. 5 g of KMnO_4 is slowly added to prevent temperature $> 20^\circ\text{C}$. It was stirred for 3 h in ice-bath and then stirred overnight for 18 h under RT. Temperature of mixture was raised to 35°C in another 30 min, with constant stirring; mixture gradually thickened into a brownish grey coloured paste. 80 mL distilled water was added into the paste in 15 min, maintaining temperature $> 80^\circ\text{C}$. Resulting solution was then cooled down to RT under tap water and preserved for another 10 min. The suspension was further diluted with distilled water to 245 mL approximately, followed by addition of 40 mL of 3% H_2O_2 ; the suspension turned bright yellow. It was filtered, resulting biscuit-coloured filter cake was washed thrice with 3% diluted HCl and warm water. Graphene oxide produced was dried for few days in vacuum.

2.2.2. Preparation of Graphene Oxide

Graphene oxide was prepared by suspending 2.5×10^{-2} g Graphite oxide in 50 mL triple distilled water and ultrasonicated for 1 h for exfoliation. The homogeneous mixture was centrifuged at 3000 rpm for 30 min to get non-sediment supernatant solution [27]. Graphene oxide obtained as the residue was washed and dried.

2.2.3. Preparation of zeolite modified electrodes:

G-foil was treated in conc. nitric acid for 1 h. Then, graphene oxide was homogeneously dispersed in a solution of 5% Nafion 117 in isopropyl alcohol and distilled water under ultrasonic irradiation for 90 min. The catalyst ink was then painted on pre-treated G-foil to cover an area of 1 cm^2 ; the other side of the foil being covered by cello-tape. Again, 1:1 mechanical mixture of graphene oxide and ZSM-5 was homogeneously dispersed in a 5% solution of Nafion 117 in 20 v/v of isopropyl alcohol and distilled water, subjected to ultrasonic irradiation for 1800 s. The catalyst ink was then painted on pre-treated G-foil to cover an area of 1 cm^2 to get the zeolite modified electrode; the other side of the foil being covered by non-conducting cello-tape. The loading of graphene oxide was approximately 5×10^{-4} g which was later used to determine the mass activity (MA) which is nothing but the current (in mA) recorded per unit mass of the loaded catalyst (in mg); the catalyst being Pt. The GO/G-foil and (GO-ZSM-5)/G-foil electrodes were dried in a desiccator overnight.

2.2.4. Electro-reduction of graphene oxide:

The G-foil was loaded with graphene oxide on one side while the other side was kept blocked by non-conducting cello-tape.

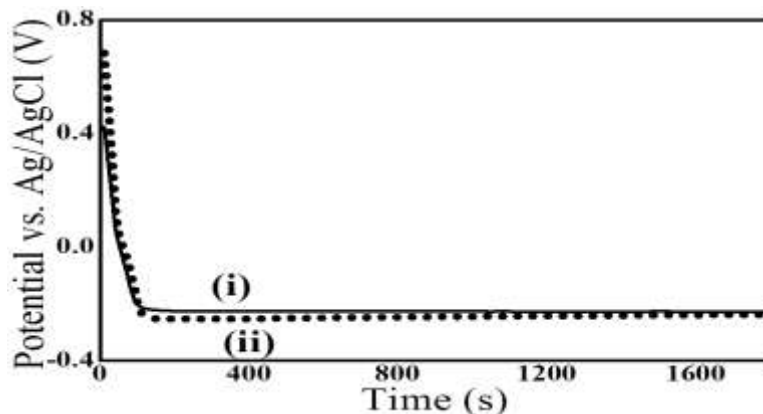


Figure 1. Electro-reduction of GO/G-foil & (GO-ZSM)/G-foil in 0.5 M H₂SO₄ at (-) 0.001 A/cm² for 1800 s.

Then graphene oxide over the G-foil surface was reduced to reduced graphene oxide electrochemically in a bath containing 0.5 M H₂SO₄ solution by passing a current density of 0.001 A/cm² for 1800 s by means of Autolab cyclic voltammeter (Figure 1). The reduced electrode washed thoroughly by triple-distilled water.

2.2.5. Electro-deposition of Platinum:

Pt was electro-deposited on the modified electrodes galvanostatically from a 2×10^{-3} M solution of chloroplatinic acid in 1.0 M H₂SO₄ by passing a current of 0.001 A/cm² for 100 s by employing Autolab cyclic voltammeter to get Pt/GO/G-foil and Pt/(GO-ZSM-5)/G-foil (Figure 2).

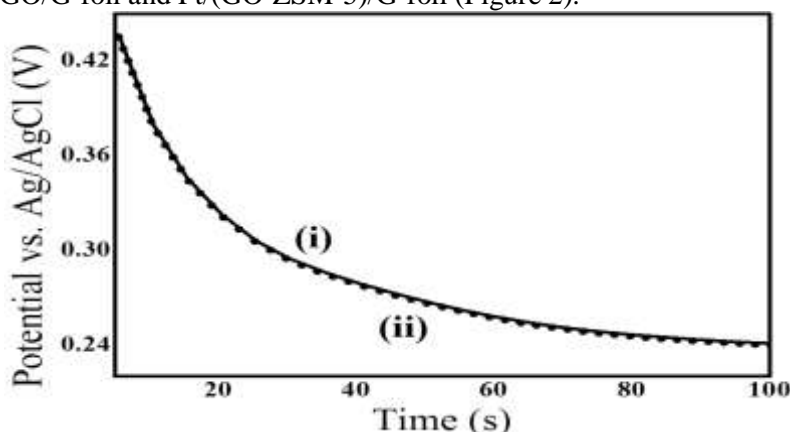


Figure 2. Electro-deposition of platinum on GO/G-foil & Pt/(GO-ZSM)/G-foil from chloroplatinic acid hexahydrate passing (-) 0.001 A/cm² current density for 100 s.

3. Characterization results:

3.1. FTIR spectrum analysis:

GO was characterized by Fourier transform infrared (FTIR) spectroscopy using Shimadzu FT-IR 8400 S (Figure 3).

The peaks at 3600 - 3400 cm⁻¹ for -OH stretching vibrations, the peak at 1739 cm⁻¹ for C = O stretching vibration, the peak at 1587 cm⁻¹ for skeletal vibration from un-oxidized graphitic domains, the peak at 1422 cm⁻¹ for aromatic C = C stretching, the peak at 1227 cm⁻¹ for C-OH stretching vibrations, 839 cm⁻¹ for epoxy group indicated the formation of GO.

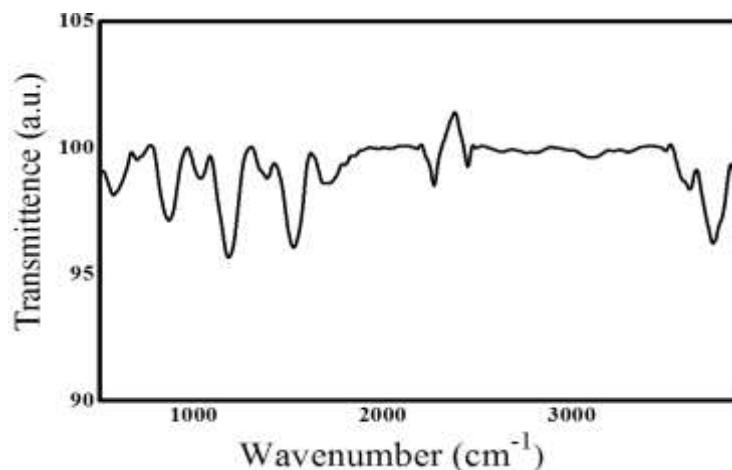


Figure 3. FTIR spectrum of GO.

3.2. Powder XRD analysis:

The Powder X-Ray diffraction (XRD) of ZSM-5 was done using Rigaku Ultima IV with Cu K α radiation ($\lambda = 0.15406$ nm) over a scanning range of $2\theta = 5 - 70^\circ$ with a step width of 0.05° , and at a voltage of 30 kV and a current of 15 mA (Figure 4).

The pattern matched with the standard diffraction pattern; the hkl peaks of (011), (020), (051), (101), (301), (501) and (503) at $2\theta = 22.99^\circ$ to 25° corresponded to the specific peaks of ZSM-5 and possessed comparable values of relative intensities as reported in the literature [28-30].

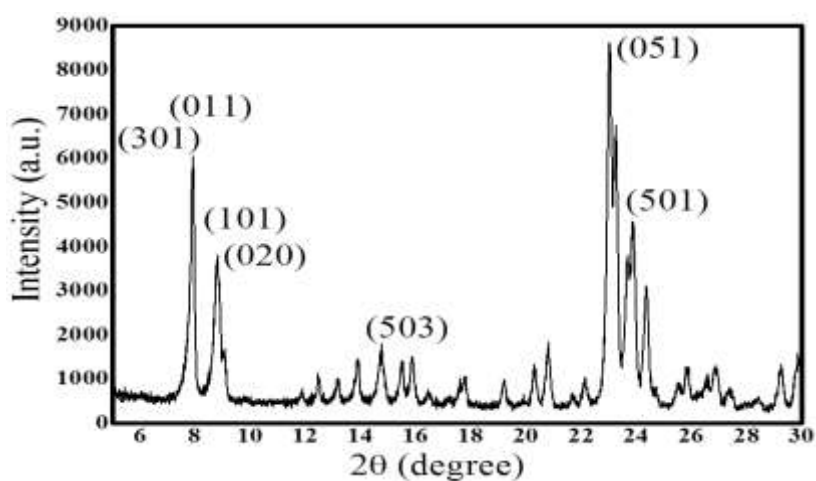


Figure 4. XRD diffractogram patterns of ZSM-5.

3.3. SEM- EDS & TEM analyses:

SEM of ZSM-5 (Figure 5i) shows the particle size of in the order of 200-250 nm which is calculated by imageJ software [31,32].

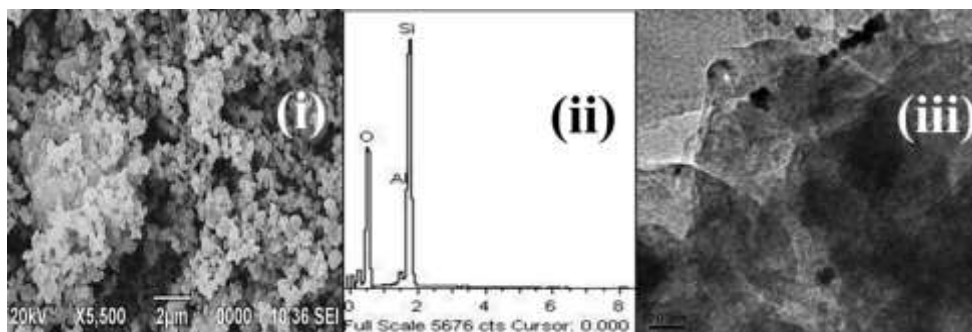


Figure 5. SEM micrograph of ZSM-5.

EDS analysis of ZSM-5 (Figure 5ii) proves the presence of all the elements of ZSM-5 and revealed that the weight percentage (wt%) of Si, Al and O in ZSM-5 were approximately 58, 20 and 22% respectively; which establishes the purity of the zeolite used in the investigation.

In the TEM micrograph, the nanoparticle size of ZSM-5 is around 200-250 nm and the sizes of PNPs deposited on Pt/ZSM-5/C are found to be below 8-10 nm as determined by imageJ software (Figure 5iii).

4. Electrochemical studies:

GO/G-foil and GO/ZSM-5/G-foil electrodes were prepared and their electro-catalytic behaviour on oxidation of 1 M ethanol in 0.5 M H₂SO₄ was investigated. Chronoamperograms of Pt/GO/G-foil and Pt/GO/ZSM-5/G-foil electrodes were done to detect the loss in current generated.

4.1. Cyclic voltammetric analyses:

The electro-oxidation of 1.0 M ethanol in 0.5 M H₂SO₄ was done on both Pt/GO/G-foil and Pt/(GO-ZSM-5)/G-foil at 0.05 V/s scan rate within the potential scan window of 0 to 1.2 V and base voltammograms of blank G-foil in 0.5 M H₂SO₄ and 1.0 M ethanol respectively (Figure 6).

In case of methanol electro-oxidation, for Pt/GO/G-foil catalysis, i_f and i_b are 324.4×10^{-4} and 261.9×10^{-4} A/cm² respectively; the ratio of i_f/i_b being 1.24. Again, for Pt/(GO-ZSM-5)/G-foil, i_f is 329.2×10^{-4} A/cm² while backward peak is insignificant.

In case of ethanol electro-oxidation, for Pt/GO/G-foil catalysis, i_f and i_b are 293.0×10^{-4} and 265.7×10^{-4} A/cm² respectively; the ratio of i_f/i_b being 1.92. Again, for Pt/(GO-ZSM-5)/G-foil, i_f is 302.1×10^{-4} while backward peak is insignificant [33].

This implies huge increase in oxidation of platinum surface into P-O_x in the presence of MCM-41 which reduces the active surface area of platinum and thus i_b is negligible compared to i_f . This could be due to the higher separation and exposure of graphene oxide as well as platinum in ZSM-5 matrix due to the inherent microporous sieve structure of the catalyst without ZSM-5.

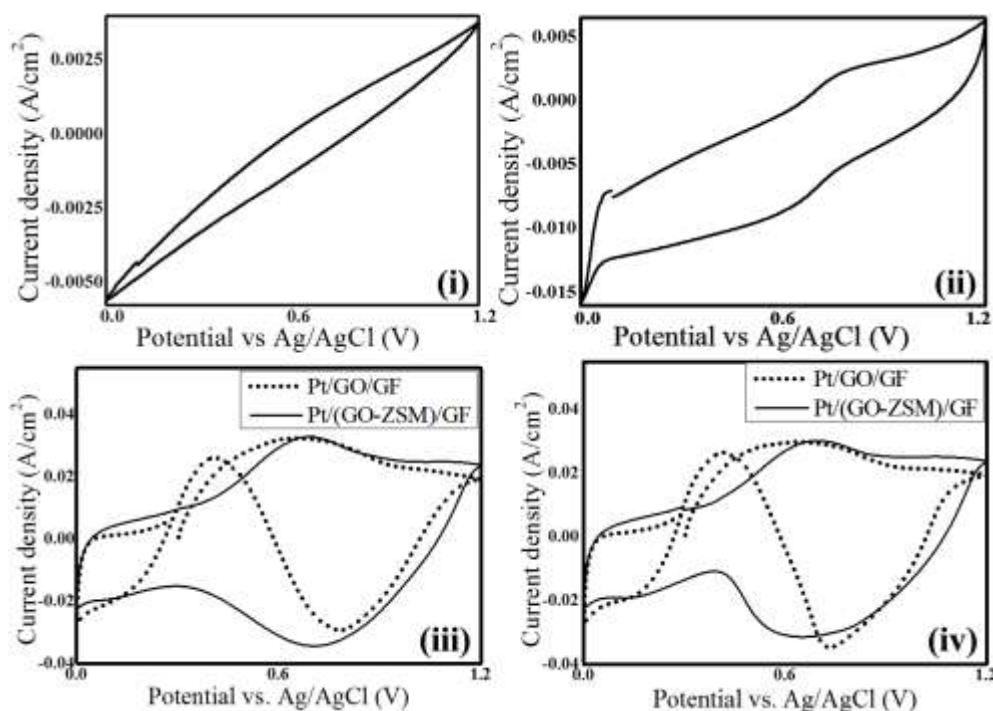


Figure 6. Base voltammograms of blank graphite foil in (i) 0.5 M H_2SO_4 , (ii) 1.0 M ethanol & 0.5 M H_2SO_4 ; Cyclic voltammograms of electro-oxidation of 1.0 M (iii) methanol & (iv) ethanol in 0.5 M H_2SO_4 at 0.05 V/s scan rate with Pt/GO/G-foil & Pt/(GO-ZSM-5)/G-foil.

It has been reported by many electrochemists that presence of Ru-OH can facilitate release of carbon dioxide from carbon monoxide by releasing proton and electron and reactivate the platinum surface [34-41]. So, the higher resistance to carbon monoxide poisoning by ZSM-5 containing modified electrode can be explained in the similar line as ZSM-5 also has hydroxyl groups in its framework that can act facilitate release of adsorbed carbon monoxide from platinum sites as carbon dioxide which clears the electrode surface for next cycle of electro-oxidation reaction mechanism.

Contrary to the earlier belief, the backward peak is not due to adsorbed carbon monoxide oxidation but due to alcohol electro-oxidation over oxidized Pt. The forward and backward peaks intersect each other as in alcohol electro-oxidation catalysed by Pt/GO/G-foil the backward peaks are prominent due to electro-oxidation of alcohols adsorbed on oxidized platinum [42].

The introduction of ZSM-5 was found to significantly accelerate the process of ethanol electro-oxidation by clearing the active sites quickly. The base voltammograms of blank G-foil in 0.5 M H_2SO_4 and 1.0 M ethanol gives the pattern of hysteresis that shows no peak in current density. In the former voltammogram in 0.5 M H_2SO_4 , no recognizable peak in current density was observed and in the latter, it was confirmed that without the presence of the acid electrolyte electro-oxidation reaction of ethanol didn't occur. This established that the i_f and i_b are produced by the electro-oxidation reaction of ethanol on the electrode surface, only in the acidic medium.

4.2. Chronoamperometric analyses:

Chronoamperograms of both the catalysts at 0.4 V were done to verify their corresponding stability (Figure 9).

Chronoamperograms of both the catalysts were comparable though the stability of Pt/(GO-ZSM)/G-foil increased than that of Pt/GO/G-foil after 2500 s which also proved that the GO-ZSM composite catalyst betters the catalyst without ZSM-5 in catalysing electro-oxidation of Ethanol. After 2500 s electrocatalysis the current density is considered to be in a steady-state.

The TON was calculated from the current density at 3500 s by using the following equation,

TON = No. of Molecules / No. of Sites

$$= (6.023 \times 10^{23} \times i) / (1.3 \times 10^{15} \times n \times F)$$

where, i is the steady-state current density at 3500 s of scanning, n is the number of electrons produced by oxidation of 1.0 M ethanol (i.e. 12), F is the Faraday constant (96,487 C), and $1.3 \times 10^{15} \text{ cm}^{-2}$ is the density of the topmost atoms of an ideal Pt(100) surface [1,43]. The TON calculated for zeolite modified electrode was found to be 520 while that for the electrode without ZSM-5 was found to be 480. This established the fact that catalytic ability increased by the introduction of ZSM-5 which again proved the positive effect of ZSM-5 in zeolite modified electrode.

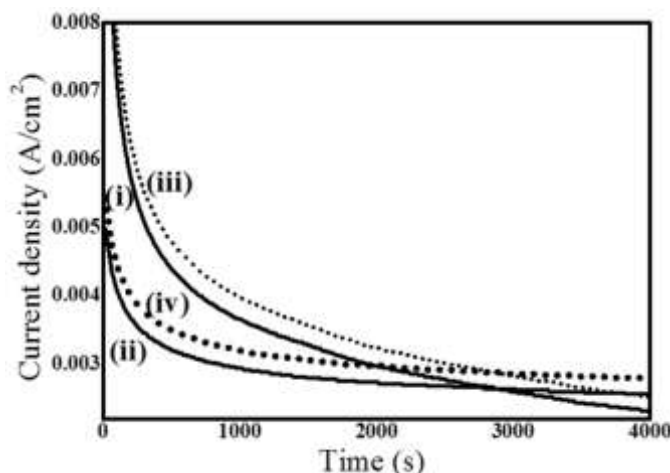


Figure 7. Chronoamperograms of (i) Pt/GO/GF & (ii) Pt/(GO-ZSM)/GF, in 1.0 M EtOH + 0.5 M H₂SO₄; and (iii) Pt/GO/GF & (iv) Pt/(GO-ZSM)/GF, in 1.0 M MeOH + 0.5 M H₂SO₄ at 0.4 V for 4000 s.

4.3. Tafel plot analyses:

In case of electro-oxidation of both MeOH and EtOH, i_{corr} for Pt/(GO-ZSM)/GF is found higher and E_{corr} is found lower than those of Pt/GO/GF.

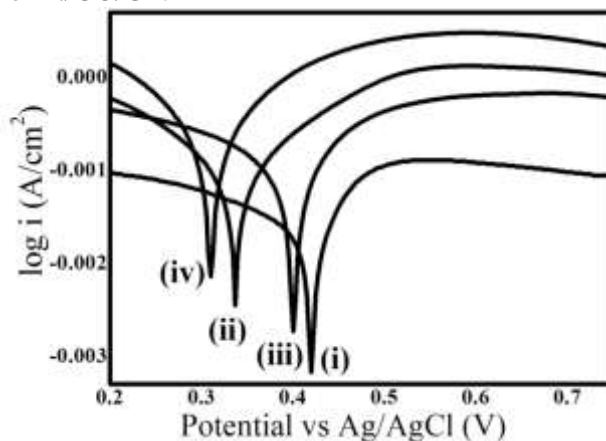


Figure 8. Tafel plots of (i) Pt/GO/GF & (ii) Pt/(GO-ZSM)/GF, in 1.0 M EtOH + 0.5 M H₂SO₄; and (iii) Pt/GO/GF & (iv) Pt/(GO-ZSM)/GF, in 1.0 M MeOH + 0.5 M H₂SO₄.

Higher i_{corr} for Pt/(GO-ZSM)/GF shows that ZSM-5 in ZMEs accelerates the electro-oxidation of both the alcohols while lower E_{corr} for Pt/(GO-ZSM)/GF shows that ZMEs facilitate electro-oxidation of both the alcohols at a lower potential; thus the process of electro-oxidation becomes easier. Again higher slope of the anodic current vs. potential curve for Pt/(GO-ZSM)/GF than that for Pt/C confirms that the former are better catalysts for the electro-oxidation of both alcohols than the latter [4].

5. Discussion & Conclusion:

From the investigation, it was found that GO modified with ZSM-5 increased electrode's resistance

towards carbon monoxide poisoning confirmed by increase in the ratio of i_p/i_b . ZSM-5 into GO functioned as a spacer to increase the separation and exposure of GO as well as the Pt active sites making the desorption of carbon dioxide much easier. Moreover, the zeolite modified electrodes were found more stable than the pure GO electrodes and also more active in the long run. Further study can be done by modification of the substrate to get higher resolution peak within lesser potential range. More ratios of GO and ZSM-5 can be tried to identify the optimum one to catalyse the electro-oxidation of both alcohols with best results.

References:

- [1]. Ye W., Zhang X., Chen Y., Du Y., Zhou F., Wang C., Pulsed electrodeposition of reduced graphene oxide on glass carbon electrode as an effective support of electrodeposited Pt microspherical particles, *Int. J. Electrochem. Sci.*, 2013, 8 (2), 2122-2139.
- [2]. Léger J.M., Rousseau S., Coutanceau C., Hahn F., Lamy C., How bimetallic electrocatalysts does work for reactions involved in fuel cells?: Example of ethanol oxidation and comparison to methanol, *Electrochim. Acta*, 2005, 50 (25-26), 5118-5125.
- [3]. Lamy C., Lima A., LeRhun V., Delime F., Coutanceau C., Léger J.M., Recent advances in the development of direct alcohol fuel cells (DAFC), *J. Power Sources*, 2002, 105 (2), 283-296.
- [4]. Pang H., Chen J., Yang L., Liu B., Zhong X., Wei X., Ethanol electrooxidation on PtZSM-5 zeolite-C catalyst, *J. Solid State Electrochem.*, 2008, 12 (3), 237-243.
- [5]. Chai G.S., Yoon S.B., Yu J., Ordered porous carbons with tunable pore sizes as catalyst supports in direct methanol fuel cell, *J. Physical Chem.*, 2004, B 108 (22), 7074-7079.
- [6]. Nam K.D., Kim T.J., Kim S.K., Lee B., Peck D.H., Ryu S.K., Jung D.H., Preparation of uniform porous carbon from mesophase pitch and its characteristics of catalyst support for the direct methanol fuel cell, *J. Korean Ind. Eng. Chem.*, 2006, 17 (2), 223-228.
- [7]. Zhu Y., Murali S., Cai W., Li X., Suk J.W., Potts J.R., Ruoff R.S., Graphene and graphene oxide: synthesis, properties, and applications, *Adv. Mater.*, 2010, 22 (35), 3906-3924.
- [8]. Geim A.K., Novoselov K.S., The rise of graphene, *Nat. Mater.*, 2007, 6, 183-191.
- [9]. Peng Z., Yang H., Designer Platinum Nanoparticles: Control of Shape, Composition in Alloy, Nanostructure and Electro catalytic Property, *Nano Today*, 2009, 4 (2), 143-164.
- [10]. Tian N., Zhou Z.Y., Sun S.G., Platinum metal catalysts of high-index surfaces: from single-crystal planes to electrochemically shape-controlled nanoparticles, *J. Phys. Chem. C*, 2008, 112 (50), 19801-19817.
- [11]. Lee I., Delbecq F., Morales R., Albiter M.A., Zaera F., Tuning selectivity in catalysis by controlling particle shape, *Nat. Mat.*, 2009, 8 (2), 132-138.
- [12]. Lee I., Morales R., Albiter M.A., Zaera F., Synthesis of Heterogeneous Catalysts with Well-Shaped Platinum Particles to Control Reaction Selectivity, *Proc. Natl. Acad. Sci. U.S.A.*, 2008, 105 (40), 15241-15246.
- [13]. Stankovich S., Dikin D.A., Dommett G.H.B., Kohlhaas K.M., Zimney E.J., Stach E.A., Piner R.D., Nguyen S.B.T., Ruoff R.S., Graphene-based composite materials, *Nature*, 2006, 442, 282-286.
- [14]. Stoller M.D., Park S., Zhu Y., An J., Ruoff R.S., Graphene-based ultracapacitors, *Nano Lett.*, 2008, 8 (10), 3498- 3502.
- [15]. Yan J., Wei T., Shao B., Ma F., Fan Z., Zhang M., Zheng C., Shang Y., Qian W., Wei F., Electrochemical properties of graphene nanosheet/carbon black composites as electrodes for supercapacitors, *Carbon*, 2010, 48 (6), 1731-1737.
- [16]. Das D., Basumallick I., Ghosh S., Methanol and ethanol electro-oxidation on to platinum loaded reduced graphene oxide surface for fuel cell application, *British J. Appl. Sci. Tech.*, 2015, 7 (6), 630-641.
- [17]. Si Y., Samulski E.T., Exfoliated graphene separated by platinum nanoparticles, *Chem. Mater.*, 2008, 20 (21), 6792-6797.
- [18]. Liang Y., Wu D., Feng X., Müllen K., Dispersion of graphene sheets in organic solvent supported by ionic interactions, *Adv. Mater.*, 2009, 21 (17), 1679-1683.
- [19]. Yang H., Li F., Shan C., Han D., Zhang Q., Niu L., Ivaska A., Covalent functionalization of chemically converted graphene sheets via silane and its reinforcement, *J. Mater. Chem.*, 2009, 19 (26), 4632-4638.
- [20]. Zu S.Z., Han B.H., Aqueous dispersion of graphene sheets stabilized by pluronic copolymers: formation of supramolecular hydrogel, *J. Phys. Chem.C*, 2009, 113, 13651-13657.
- [21]. Gómez-Navarro C., Weitz R.T., Bittner A.M., Scolari M., Mews A., Burghard M., Kern K., Electronic

- Transport Properties of Individual Chemically Reduced Graphene Oxide Sheets, *Nano Lett.*, 2007, 7 (11), 3499-3503.
- [22]. Yoo E., Kim J., Hosono E., Zhou H.S., Kudo T., Honma I., Large reversible Li storage of graphene nanosheet families for use in rechargeable lithium ion batteries, *Nano Lett.*, 2008, 8 (8), 2277-2282.
- [23]. Shervedani R.K., Amini A., Carbon black/sulfur-doped graphene composite prepared by pyrolysis of graphene oxide with sodium polysulfide for oxygen reduction reaction, *Electrochim. Acta*, 2014, 142, 51-60.
- [24]. Li Y., Li Y., Zhu E., McLouth T., Chiu C.Y., Huang X., Huang Y., Stabilization of high-performance oxygen reduction reaction Pt electro catalyst supported on reduced graphene oxide/carbon black composite, *JACS*, 2012, 134 (30), 12326-12329.
- [25]. Zhang J., Xie Z., Li W., Dong S., Qu M., High-capacity graphene oxide/graphite/carbon nanotube composites for use in Li-ion battery anodes, *Carbon*, 2014, 74, 153-162.
- [26]. Zhang J., Cao H., Tang X., Fan W., Peng G., Qu M., Graphite/graphene oxide composite as high capacity and binder-free anode material for lithium ion batteries, *J. Power Sources*, 2013, 241, 619-626.
- [27]. Hummers Jr. W.S., Offeman R.E., Preparation of graphitic oxide, *JACS*, 1958, 80, 1339-1339.
- [28]. Choi E., Han T.H., Hong J., Kim J.E., Lee S.H., Kim H.W., Kim S.O., Noncovalent functionalization of graphene with end-functional polymers, *J. Mater. Chem.*, 2010, 20 (10), 1907-1912.
- [29]. Morales-Pacheco P., Alvarez-Ramirez F., Angel P.D., Bucio L., Dominguez J.M., Synthesis and structural properties of zeolytic nanocrystals I. MFI type zeolites, *J. Phys. Chem. C*, 2007, 111 (6), 2368-2378.
- [30]. Treacy M.M.J., Higgins J.B., *Collection of Simulated XRD Powder Patterns for Zeolites*, Elsevier, Amsterdam, 2001, 477-485.
- [31]. Razavian M., Fatemi S., Synthesis and evaluation of seed-directed hierarchical ZSM-5 catalytic supports: inductive influence of various seeds and aluminosilicate gels on the physicochemical properties and catalytic dehydrogenative behavior, *Mater. Chem. Phys.*, 2015, 165, 55-65.
- [32]. Jamalzadeh Z., Haghghi M., Asgari N., Synthesis, physicochemical characterizations and catalytic performance of Pd/carbon-zeolite and Pd/carbon-CeO₂ nanocatalysts used for total oxidation of xylene at low temperatures, *Front. Environ. Sci. Eng.*, 2013, 7 (3), 365-381.
- [33]. Daas B.M., Das D., Ghosh S., Ethanol electro-oxidation by Pt/r(GO-ZSM)/Graphite foil, *Adv. Mat. Proc.*, 2016, 1 (2), 156-160.
- [34]. Lee M.J., Kang J.S., Kang Y.S., Chung D.Y., Shin H., Ahn C., Park S., Kim M., Kim S., Lee K., Sung Y., Understanding the bifunctional effect for removal of CO poisoning: blend of platinum nanocatalyst and hydrous ruthenium oxide as a model system, *ACS Catal.*, 2016, 6, 2398-2407.
- [35]. Mojović Z., Mudrinić T., Rabi-Stanković A.A., Ivanović-Šašić A., Marinović S., Zunić M., Jovanović D., Methanol Electrooxidation on PtRu Modified Zeolite X, *Sci. Sinter.g* 45 2013 89-96.
- [36]. Chung D.Y., Kim H., Chung Y., Lee M.J., Yoo S.J., Bokare A.D., Choi W., Sung Y., Inhibition of CO poisoning on Pt catalyst coupled with the reduction of toxic hexavalent chromium in a dual-functional fuel cell, *Sci.Rep.*, 2014, 4, 7450-7454.
- [37]. Li L., Xing Y., Methanol electro-oxidation on Pt-Ru alloy nanoparticles supported on carbon nanotubes, *Energies*, 2009, 2, 789-804.
- [38]. Iwasita T., Electrocatalysis of methanol oxidation, *Electrochim.Acta* 47 2002 3663-3674.
- [39]. Fernanda G., Medeiros R.S., Jean G.E., Lucia G.A., Active sites for ethanol oxidation over SnO₂-supported molybdenum oxides, *Appl. Catal. A Gen.*, 2000, 193, 195-202.
- [40]. Friedrich K.A., Geyzers K.P., Linke U., Stimming U., Stumper J., CO adsorption and oxidation on a Pt(111) electrode modified by ruthenium deposition: An IR spectroscopic study, *J. Electroanal. Chem.*, 1996, 402 (1-2), 123-128.
- [41]. Watanabe M., Motoo, Electrocatalysis by ad-atoms: part III. Enhancement of the oxidation of carbon monoxide on platinum by ruthenium ad-atoms, *J. Electroanal. Chem. Interfacial Electrochem.*, 1975, 60 (3), 275-283.
- [42]. Chung D.Y., Lee K.J., Sung Y.E., Methanol electro-oxidation on the Pt surface - revisiting the cyclic voltammetry interpretation, *J. Phys. Chem. C*, 2016, 120, 9028-9035.
- [43]. Singh A., Quraishi M.A., Pipali (Piper longum) and Brahmi (Bacopa monnieri) extracts as green corrosion inhibitor for aluminum in NaOH solution, *J Chem Pharm Res.*, 2012, 4 (1), 322-325.
